SINTEF
PROCEEDINGS
2

Proceedings of the 12th International Conference on Computational Fluid Dynamics in the Oil & Gas, Metallurgical and Process Industries

Progress in Applied CFD – CFD2017

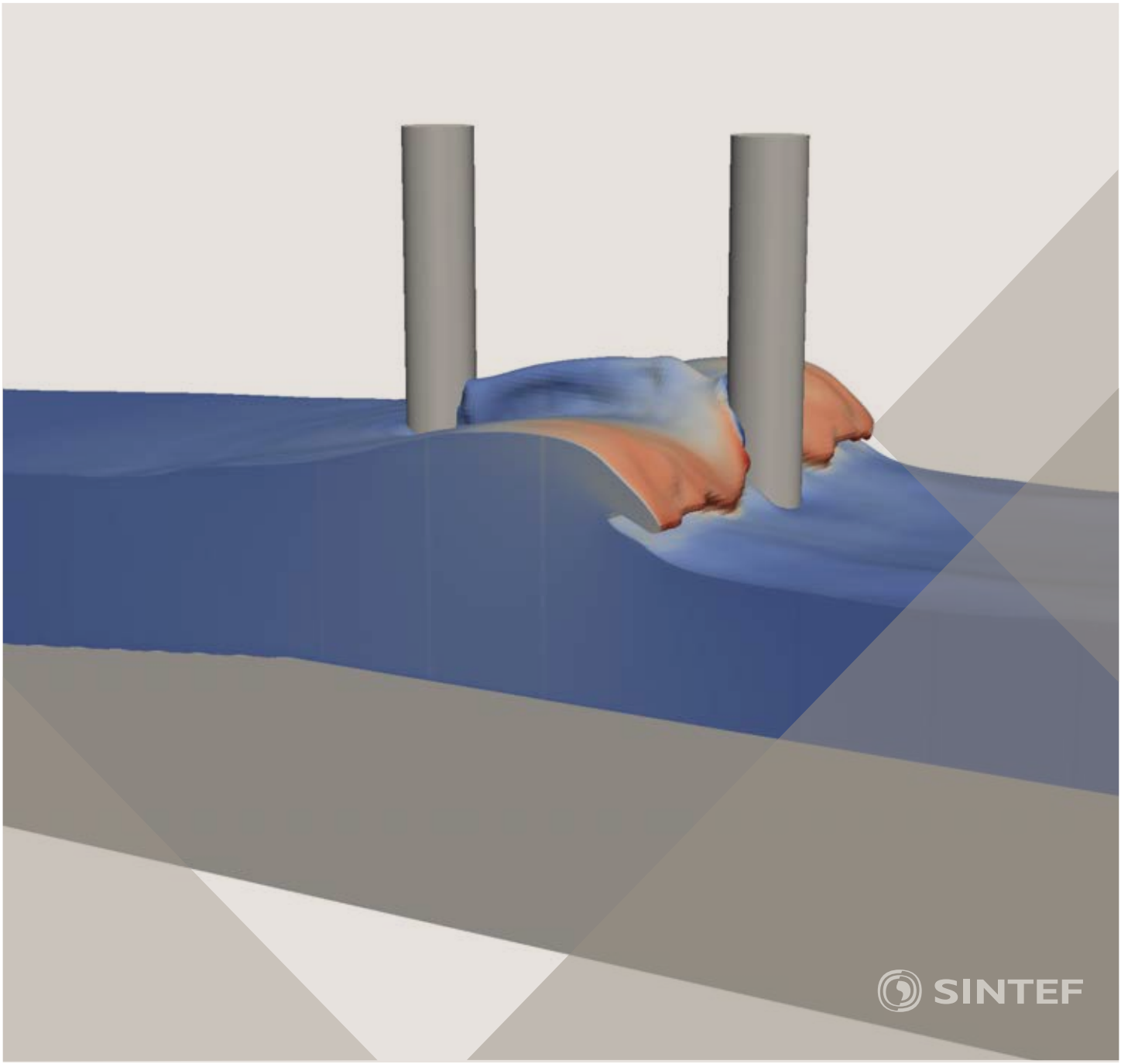

SINTEF Proceedings

Editors:
Jan Erik Olsen and Stein Tore Johansen

Progress in Applied CFD – CFD2017

Proceedings of the 12th International Conference on Computational Fluid Dynamics in the Oil & Gas, Metallurgical and Process Industries

SINTEF Academic Press

SINTEF Proceedings no 2
Editors: Jan Erik Olsen and Stein Tore Johansen
Progress in Applied CFD – CFD2017
Selected papers from 10th International Conference on Computational Fluid Dynamics in the Oil & Gas, Metallurgical and Process Industries

Key words:
CFD, Flow, Modelling

Cover, illustration: Arun Kamath

ISSN 2387-4295 (online)
ISBN 978-82-536-1544-8 (pdf)

SINTEF Academic Press
Address: Forskningsveien 3 B
PO Box 124 Blindern
N-0314 OSLO
Tel: +47 73 59 30 00
Fax: +47 22 96 55 08

www.sintef.no/byggforsk
www.sintefbok.no

SINTEF Proceedings
SINTEF Proceedings is a serial publication for peer-reviewed conference proceedings on a variety of scientific topics.
The processes of peer-reviewing of papers published in SINTEF Proceedings are administered by the conference organizers and proceedings editors. Detailed procedures will vary according to custom and practice in each scientific community.

PREFACE

This book contains all manuscripts approved by the reviewers and the organizing committee of the 12th International Conference on Computational Fluid Dynamics in the Oil & Gas, Metallurgical and Process Industries. The conference was hosted by SINTEF in Trondheim in May/June 2017 and is also known as CFD2017 for short. The conference series was initiated by CSIRO and Phil Schwarz in 1997. So far the conference has been alternating between CSIRO in Melbourne and SINTEF in Trondheim. The conferences focuses on the application of CFD in the oil and gas industries, metal production, mineral processing, power generation, chemicals and other process industries. In addition pragmatic modelling concepts and bio-mechanical applications have become an important part of the conference. The papers in this book demonstrate the current progress in applied CFD.

The conference papers undergo a review process involving two experts. Only papers accepted by the reviewers are included in the proceedings. 108 contributions were presented at the conference together with six keynote presentations. A majority of these contributions are presented by their manuscript in this collection (a few were granted to present without an accompanying manuscript).

The organizing committee would like to thank everyone who has helped with review of manuscripts, all those who helped to promote the conference and all authors who have submitted scientific contributions. We are also grateful for the support from the conference sponsors: ANSYS, SFI Metal Production and NanoSim.

Stein Tore Johansen & Jan Erik Olsen

Organizing committee:

Conference chairman: Prof. Stein Tore Johansen
Conference coordinator: Dr. Jan Erik Olsen
Dr. Bernhard Müller
Dr.Sigrid Karstad Dahl
Dr.Shahriar Amini
Dr.Ernst Meese
Dr.Josip Zoric
Dr.Jannike Solsvik
Dr.Peter Witt

Scientific committee:

Stein Tore Johansen, SINTEF/NTNU
Bernhard Müller, NTNU
Phil Schwarz, CSIRO
Akio Tomiyama, Kobe University
Hans Kuipers, Eindhoven University of Technology
Jinghai Li, Chinese Academy of Science
Markus Braun, Ansys
Simon Lo, CD-adapco
Patrick Segers, Universiteit Gent
Jiyuan Tu, RMIT
Jos Derksen, University of Aberdeen
Dmitry Eskin, Schlumberger-Doll Research
Pär Jönsson, KTH
Stefan Pirker, Johannes Kepler University
Josip Zoric, SINTEF

CONTENTS

CFD BASED STUDY OF DENSE MEDIUM DRUM SEPARATION PROCESSES

Arne EGGERS[1]*, **Wim DEWULF**[1†], **Martine BAELMANS**[1‡], **Maarten VANIERSCHOT**[1§]

[1]KU Leuven Mechanical Engineering Department , 3000 Leuven , BELGIUM

* E-mail: arne.eggers@kuleuven.be
† E-mail: wim.dewulf@kuleuven.be
‡ E-mail: martine.baelmans@kuleuven.be
§ E-mail: maarten.vanierschot@kuleuven.be

ABSTRACT

Dense Medium Drum (DMD) separation is applied particularly in the coal and recycling industries. Characteristic of the process is a separation based on density, driven by the buoyancy and gravitational forces acting on an object moving in a free surface flow. The fundamental phenomena occurring in a DMD have been widely investigated by (Napier-Munn, 1991). However, in contrary to other separation methods, such as the Dense Medium Cyclone which was investigated extensively by (Kuang *et al.*, 2014) and others, no Computational Fluid Dynamics (CFD) studies have been conducted for the DMD separation. Even recent studies, like (Meyer and Craig, 2015), use first order models which need to be calibrated with performance data of the investigated drum. Hence, important parameters like the flow-velocity and the detailed design of the drum are only taken into account indirectly.

This paper reports a detailed CFD analysis of the flow in a generic DMD separation process. The study comprises, a general understanding of the flow field and an analysis of the impact of different process parameters. Furthermore, the model predicts the actual separation performance of the DMD at different working points. To the authors' knowledge, this is the first study which conducts a CFD analysis of a DMD separation process. Therefore, findings concerning the flow field and its influence on the separation efficiency will be reported on. Moreover, the separation model can be used to derive the coefficients for highly used first order models without the need of experimental data. Like this, the early design phase of DMD separation processes can improve immensely.

Keywords: CFD, Process industries, separation, free surface flow
.

NOMENCLATURE

Greek Symbols

ε	Relative error, $[-]$
η	Separation efficiency, $[-]$
μ	Kinematic viscosity, $[m^2/s]$
ρ	Mass density, $[kg/m^3]$
ϕ	Medium volume fraction, $[-]$
ω	Turbulent Frequency, $[1/s]$

Latin Symbols

C_D	Drag Coefficient, $[-]$.
d	Diameter, $[m]$.
dir	Direction, $[-]$.
F	Force, $[N]$.
F_s	Safety coefficient for the GCI, $[-]$.
g	Gravitational acceleration, $[m/s^2]$.
GCI	Grid convergence index, $[-]$.
k	Turbulent Kinetic Energy, $[m^2/s^2]$.
m	Mass, $[kg]$.
n	Number of objects, $[-]$.
p	Pressure, $[Pa]$.
po	Order of grid convergence, $[-]$.
r	Grid refinement factor, $[-]$.
Re	Reynolds number, $[-]$.
t	Time, $[s]$.
T	Viscous stress tensor, $[N/m^2]$.
u	Velocity, $[m/s]$.
V	Volume, $[m^3]$.
x	Location, $[m]$.

Sub/superscripts

B	Buoyancy,
c	Carrier fluid,
cg	Coarse grid,
D	Drag,
eff	Effective.
i	Index i.
j	Index j.
p	Particle or Object.
$turb$	Turbulent.
r	Relative.

INTRODUCTION

In the environmental action plan for the circular economy, the European Union sets ambitious targets for recycling rates. This makes the development and optimization of current recycling processes mandatory. Dense Medium Drums (DMDs) are density separation machines frequently used in the coal and the recycling industry. In general the medium is a suspension of a high density powder with water. As illustrated in figure 1, objects with a density lower than the medium density float and leave the drum on the surface through the light fraction outlet. Other objects sink and are extracted from the drum by collectors or spirals which are driven by the rotation of the drum. Medium is supplied through inlet tubes and a small angle of inclination assures a constant stream towards the light fraction outlet of the drum. Although the coal industry applies DMD separation already for several decades, the approaches of modeling the process are restricted to first order models which get tuned by measurement data (Napier-Munn, 1991). These models predict for instance the behavior of the Wemco Drum, taking

different diameters of the separation objects into account (P.J. Baguley and T.J. Napier-Munn, 1996). The modeling of sub-processes like the DMD is accompanied by macroscopic analyses of the complete process in a plant (King, 1999). Furthermore, a recent study improves the modeling approaches by proposing a method, based on solving a system of differential equations, designed to be applied in the control of DMDs (Meyer and Craig, 2015). None of these studies directly investigates the flow in the drum and its influence on the separation process. This can only be achieved by utilizing experimental technics or Computational Fluid Dynamics (CFD). DMDs for the application of plastic separation have been investigated experimentally (Dodbiba *et al.*, 2002). However, none of these studies applies CFD. CFD enables the possibility to base models for the design of DMDs on the flow simulation. This makes an optimization of the actual process during the design phase possible.

The modeling of a DMD based on CFD can be divided into two different major problems: The simulation of the free surface flow and the modeling of separation objects. Free surface flow simulation make currently mainly use of two models. The level-set method tracks the surface, directly storing its position in a distance field (Stanley Osher and James A. Sethian, 1988). Hence, a sharp interface is conserved. The second method makes use of the volume of fluid (VOF) method (C. W. Hirt and B.D. Nichols, 1981). One of the phases is marked using a coloring function which is advected passively with the local flow field. The interface is not necessarily sharp. To estimate its exact position an interface reconstruction, based on the distribution of the color function, is needed.

The modeling of the objects in flows can be characterized by its description of the object domain. Objects which are considered to be large compared to the grid cell size have to be resolved and simulated. These methods are physically accurate, on the one hand, but computationally expensive, on the other (G. Houzeaux *et al.*, 2010). Smaller objects, often referred to as particles, can be described as point mass (Dehbi, 2008). This makes the modeling of huge amounts of objects with reasonable computational costs possible.

In the present research a generic DMD will be simulated. The free surface is modeled using the VOF method (Omno Ubbink, 1997). Although the separation objects are considered to be large, the model describes them as point masses. To prevent nonphysical flow behavior due to the large point masses a one-way coupling, which neglects the influence of the objects onto the flow, is applied. Thus, the separation performance of the generic drum in dependency of different flow parameters can be estimated.

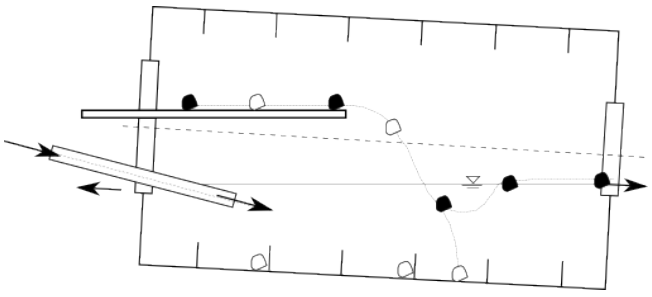

Figure 1: Sketch of a generic DMD.

MODEL DESCRIPTION

The model has been implemented into the existing framework of the OpenFOAM toolbox. Hence, all equations and models described below are solved using this toolbox. The incompressible Reynolds averaged Navier-Stokes (RANS) equations are solved,

$$\frac{\partial \bar{u}_i}{\partial x_j} = 0, \tag{1}$$

$$\frac{\partial \bar{u}_i}{\partial t} + \bar{u}_j \frac{\partial \bar{u}_i}{\partial x_j} = -\frac{1}{\rho}\frac{\partial \overline{p}}{\partial x_i} + \frac{\partial}{\partial x_j}\left(\frac{1}{\rho}T_{ij} - \overline{u_i' u_j'}\right) + g_i. \tag{2}$$

As these equations on their own are not closed, a k-ω SST model is applied to model the Reynolds stress tensor and the turbulent viscosity. This model solves an extra set of equations for the turbulent kinetic energy and the turbulent frequency. A detailed description of it can be found in the literature (Menter, 1994). A finite volume scheme with a first order upwind interpolation was used for the spacial discretization. For the time derivation an Euler forward scheme has been applied.

In the investigated generic drum geometry the medium is a suspension out of Ferro Sillicon powder and water. The model assumes that the powder and the water is in perfect suspension at any place and time and hence behaves as one continuum with constant fluid dynamical properties. The VOF method models the free surface between the air phase and the medium phase in the drum (Omno Ubbink, 1997). A color function ϕ is utilized which indicates the volume proportion of the medium phase at a certain location of the drum. $\phi = 1$ in the medium phase, $\phi = 0$ in the air phase and $0 < \phi < 1$ in the interface area. The color function advects passively with local flow field,

$$\frac{\partial \phi}{\partial t} + \bar{u}_j \frac{\partial \phi}{\partial x_j} = 0. \tag{3}$$

Object Tracking

The Lagrangian equations of motion describe the movement of the objects in the flow,

$$\frac{dx_{p,i}}{dt} = u_{p,i}, \tag{4}$$

$$\frac{du_{p,i}}{dt} = \frac{1}{m_p}(F_{D,i} + F_{B,i}). \tag{5}$$

The summed forces in equation 5 consist out of two contributions: the drag force and the buoyancy force. Equation 5 is integrated using a first order explicit Euler scheme. The forces are modeled as described in the following.

Buoyancy Force

The difference in density between the objects and carrier fluids introduces a buoyancy force which drives the separation of the objects. The buoyancy force can be calculated,

$$F_{B,i} = \rho_p \cdot V_p \cdot g_i \cdot \left(1 - \frac{\rho_c}{\rho_p}\right). \tag{6}$$

Drag Force

The drag force is modeled based on a drag coefficient,

$$F_{D,i} = \frac{1}{2} \cdot C_D(Re_p) \cdot |u_{r,i}| \cdot u_{r,i} \cdot A_p. \tag{7}$$

Here $u_{r,i}$ is the relative velocity between the local flow field and the object. Re_p is defined as the particle Reynolds number,

$$Re_p = \frac{|u_{r,i}| \cdot d_p}{\mu}. \quad (8)$$

The drag coefficient of a sphere can be estimated,

$$C_D(Re) = \begin{cases} 0.424, & \text{if } Re \geq 1000 \\ 24(1+0.15 \cdot Re^{0.678}), & \text{otherwise} \end{cases}. \quad (9)$$

Equation 7 computes the forces acting on an object based on the averaged flow field from the solution of the RANS equations. As stated in previous studies one of the major influences on the separation process are the turbulent fluctuations of the flow which effects the objects in a stochastic way (P.J. Baguley and T.J. Napier-Munn, 1996). The computed averaged flow does not include any information about these fluctuations. However, the k-ω SST turbulence model conserves turbulent quantities, namely the turbulent kinetic energy and the turbulent frequency, which can be used to model the influence of the fluctuation statistically. Here, this is done using a popular Eddy Interaction Model (EIM) (Gosman and loannides, 1983). Without taking the turbulent fluctuations into account, objects with a density higher than the medium will get sorted as heavy fraction and all others as light fraction, if the drum is sufficiently large and the velocities small.
If an object enters the domain the forces are summed up and equation 5 is integrated. However, before the drag force is computed the turbulent fluctuations are added to the local velocity to calculate the effective local velocity,

$$u_{eff,i} = u_i + u_{turb,i}. \quad (10)$$

The magnitude of the turbulent fluctuations is sampled from a Gaussian normal distribution, with an expectation value of 0 and a standard deviation of 1, and scaled with the expected magnitude,

$$|u_{turb,i}| = \sqrt{\frac{2k}{3}} \cdot Gauss(0,1). \quad (11)$$

Turbulence models, as the applied k-ω SST model, utilizes an eddy viscosity hypothesis. As such, it assumes homogeneous turbulence. Hence, the same assumption is applied for the turbulent dispersion modeling leading to randomly sampled turbulent fluctuation,

$$dir_{turb,i} = \begin{bmatrix} rnd() \\ rnd() \\ rnd() \end{bmatrix} \text{ with } |dir_{turb,i}| = 1. \quad (12)$$

The turbulent fluctuation velocity can now be estimated,

$$u_{turb,i} = |u_{turb,i}| \cdot dir_{turb,i}. \quad (13)$$

This process samples a new turbulent velocity when equation 5 has been integrated for the duration of one turbulent time scale,

$$t_{turb} = \frac{1}{\omega}. \quad (14)$$

Coupling

Although the objects in this model are considered to be large, they are still modeled as spherical point masses. As such a drag coefficient can model the influence from the flow onto the object and the simulation of large amounts of objects is enabled. Several models exist to account for the influence from the objects onto the flow. However none of them can cope with large objects experiencing directional forces. Hence, this model utilizes, in a first pragmatic approach, a one-way coupling.
This might be a too strong assumption for a accurate simulation of the flow in the drum. However, the model is designed to deliver a reliable prediction of the separation efficiency of a DMD. In this context the assumption might be accurate enough. The algorithm updates the positions of the objects at first and then solves the flow and turbulence equations.

Separation Performance

In classical separation modeling first order models generate separation curves. These curves describe the separation number, the probability that an object gets separated as heavy or light in dependency of the object density or its theoretical terminal velocity.
To achieve these curves based on a CFD calculation the paths of a huge amount of objects have to be tracked. The number of objects leaving the drum through the light and the heavy fraction outlet can be used to calculate the separation efficiency,

$$\eta_{heavy} = \frac{n_{heavy\ outlet}}{n_{heavy\ outlet} + n_{light\ outlet}}, \quad (15)$$

$$\eta_{light} = \frac{n_{light\ outlet}}{n_{heavy\ outlet} + n_{light\ outlet}}. \quad (16)$$

For these equations it is assumed that all objects are supposed to be heavy fraction, in case of equation 15, or light fraction, in case of equation 16, independently from their density and the medium density. The efficiency is assumed to be converged if the statistical error is below 0.1%.

RESULTS

In this study a generic drum geometry is simulated and its performance is predicted for different densities and object diameters. For the calculation of the separation efficiency it is assumed that all objects are supposed to be sorted as heavy fraction. Hence, equation 15 is utilized. Based on these results separation curves for different object diameters are computed. Furthermore, a grid study is conducted and the medium flow field is investigated.

Geometry

Major dimensions and a general overview on the geometry are given in figure 2. It is a simplified, generic version of a real applied drum. No collectors for the heavy fraction objects are taken into account and the drum is not rotating. The separation zone of the drum is long enough to ensure a sufficient residence time. The whole lower part of the inlet side, in figure 2 marked as a and b, is defined as medium inlet. Here medium enters the drum with a low velocity generating a slow and steady inflow. Separation objects are released through the middle part of the inflow section, in figure 2 marked as b. The complete curved wall of the drum, in figure 2 marked as d, is defined as heavy fraction outlet. Through this outlet only separation objects but no medium can leave the drum. On the outlet side of the drum the higher light fraction outlet is located, in figure 2 marked as c. This outlet allows medium and objects to leave the drum.

Computational Grid

The computational grid, which is shown in figure 3, consists of 344640 cells. This structured grid is used for performance predictions. For the grid study a second grid with 849216 grid cells has been used.

Grid Study

For the grid study two grids are used. At first the two flow fields of the medium phase are compared and then their influence onto the separation efficiency is assessed.

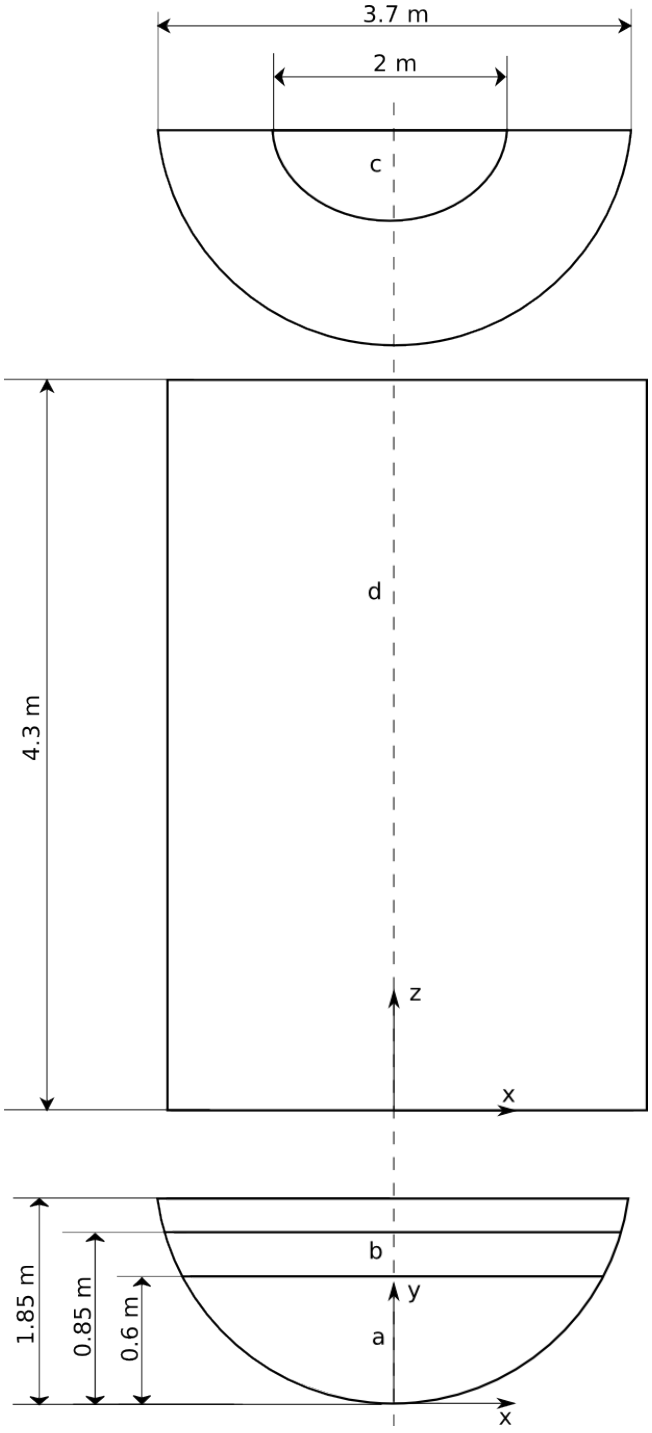

Figure 2: Sketch of the computational domain. With views on the light fraction outlet (c) (top), on the heavy fraction outlet (d) (middle), on the water inlet (a) and on the water objects mixture inlet (b) (bottom).

Medium Flow Field

In figure 4 the medium velocity profiles in the symmetry plane of the drum (x=0) are compared. After the medium enters the drum a steady flow field with a maximum velocity of approximately $u_z = 0.25\frac{m}{s}$ develops. In this area the solutions of both grids align very well and can be considered grid independent.
However, this changes as the medium passes through the drum and gets influenced by the outlet of the drum. Compared to the fine grid, the coarse grid underpredicts the outlet vortex and hence the back flow area in the lower part of the drum is smaller. Furthermore, the fine grid predicts a slightly higher peak velocity at the outlet.

Separation Efficiency

The grid convergence of the separation efficiency is assessed using the grid convergence index (GCI) (P. J. Roache, 1994),

$$GCI_{cg} = \frac{F_s \cdot |\varepsilon| \cdot r^{po}}{r^{po} - 1}. \tag{17}$$

The grid refinement factor is $r = 3$, the safety coefficient is $F_s = 3$ and the order of grid convergence is assumed to be $p = 2$. The results are summarized in table 1. Although the medium flow field differs between the two grids, the GCI for the separation efficiency remains low. Hence, the separation efficiency can be examined using the coarsest grid. The GCI drops with increasing object density as the the buoyancy forces increase while the drag force remains constant. The grid study has been conducted only for objects with a diameter of $d = 0.005$. It is expected that the grid influence is bigger for smaller objects as in these cases the grid independent buoyancy force is less important compared to the drag force.

Medium Flow Field

The medium is entering the drum through the lower part of the inlet side, which is visible in figure 2 (a and b). The inlet velocity is defined to be $u_{in} = 0.1\frac{m}{s}$. The combination of a large inlet area and a low velocity generates a slow and steady flow in the drum.

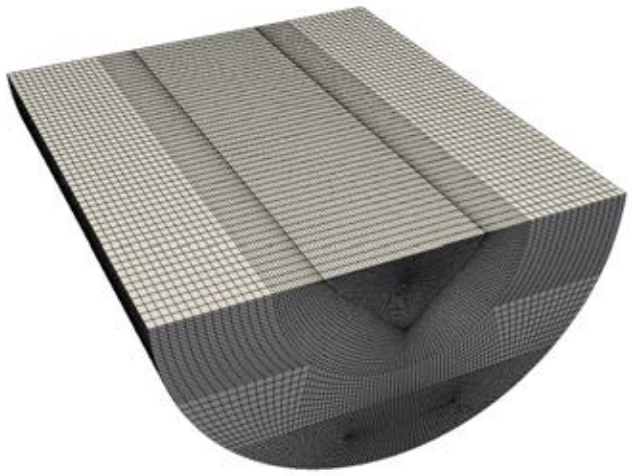

Figure 3: The computational grid used for the performance prediction.

Table 1: GCI and error in mean for objects of diameter $d = 0.005$ and different densities.

Density (kg/m^3)	GCI (%)	error in mean
900	0.0	1.348e-05
990	2.531	5.07e-05
1000	1.635	0.0002
1020	0.329	0.0003
1030	0.075	0.0002

The smaller outlet drives an acceleration of the medium. As shown in figure 5, a vortex is created under the outlet. Separation objects which do not leave the drum through the light fraction outlet get dragged towards the heavy fraction outlet by this vortex. The acceleration is strongest in the symmetry plane (x=0) and gets less in the side planes of the drum. The same trend is observed for the outlet vortex.

Performance Prediction

For the prediction of the separation performance of the generic geometry, depending on the flow and object properties, multiple hundred thousand of objects have to be traced on their path through the drum.
Figure 6 shows a typical convergence curve of the separation efficiency. The efficiency, which is calculated based on equation 15, starts with a value of one, as separation objects enter the drum over its full width. Hence, a small number of objects enter the computational domain close to the heavy fraction outlet and an even smaller amount gets dragged through it. As objects need approximately 15 seconds to pass the drum, no objects leave through the light fraction outlet at this point and an efficiency of one is computed. However, it drops as soon as objects reach the light fraction outlet. Once the outflow of objects through the heavy and light fraction outlet stabilizes at a constant value, the computed separation efficiency will converge to a statistically constant value as well. As no object-object interactions and no back-coupling from the objects onto the flow have been taken into account, the mass flow of separation objects does not influence the predicted efficiency. The case shown in figure 6 reaches convergence approximately after 80 seconds and more than 500000 tracked objects. A simulation like this predicts a separation efficiency for a specified object density and diameter. Hence,

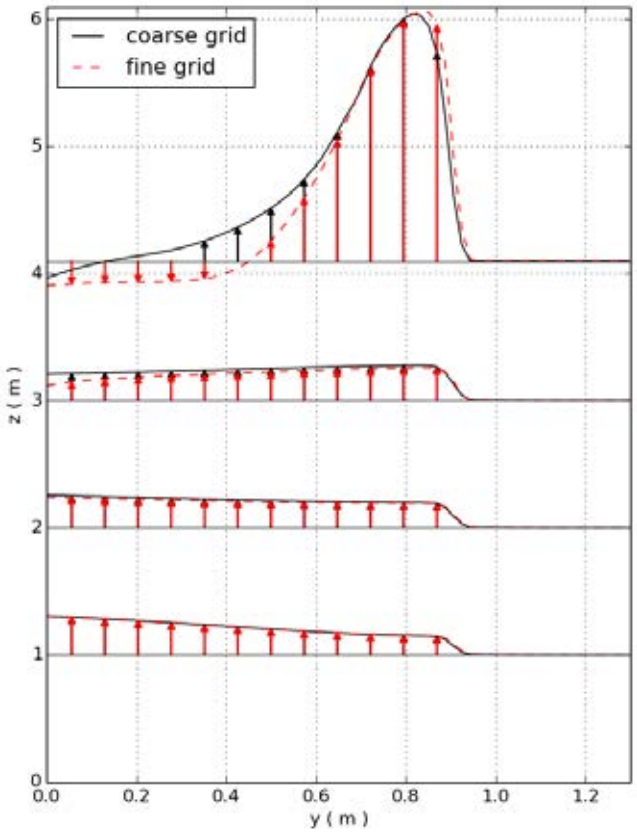

Figure 4: Medium velocity profiles in the symmetry plane (x=0) of the drum on the fine and the coarse mesh.

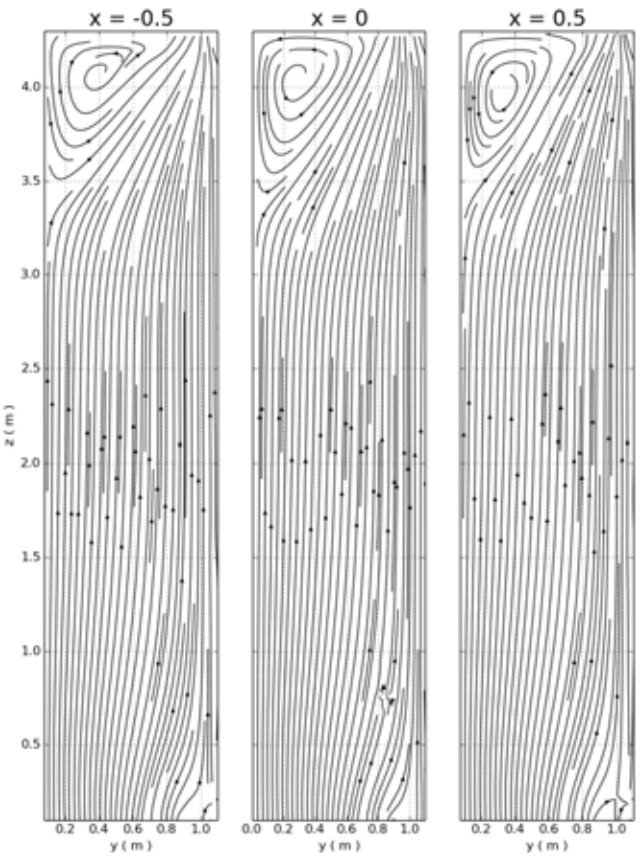

Figure 5: Streamlines in three different planes in the medium zone of the drum. The outlet is in the top (z=4.3) and the inlet in the bottom (z=0) of the figure.

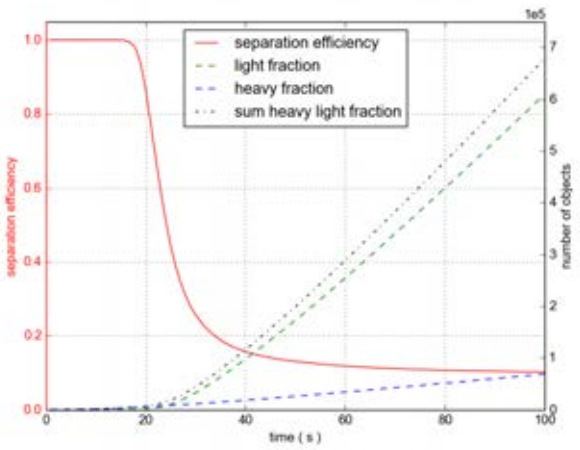

Figure 6: Computed separation efficiency and number of objects, which left the drum, over simulated time.

it delivers one point in a separation curve. If simulations are conducted for different densities and diameters the whole separation curve can be predicted.

Figure 7 shows the predicted partitioning curves for the generic geometry of different object diameters. The typical S-shape and the influence of the object diameter size is recognizable in the same way as in figure 8. Furthermore, the generic drum slightly tends to separate objects as light fraction, although their density is higher than the medium density. This is due to the high medium mass flow which accelerates towards the outlet. However, particularly for the larger object diameters the generic drum has a high separation efficiency, which leads to a very sharp S-shape of the partitioning curve. For smaller objects the influence of the buoyancy force, which drives the separation, becomes less dominant compared to the drag force. Hence, the separation efficiency for these cases are much lower and the S-shape is more blurry.

CONCLUSION

A CFD based model, which predicts the separation efficiency of a DMD has been proposed. It has been applied to a generic and simplified drum geometry. As the CFD simulations deliver information on the general flow field in the drum, this has been investigated as well and key structures like the outlet vortex have been discussed.

The model reproduces the characteristic S-shape of separation curves for DMDs including its trend for objects with different size. Hence, in a next step a real DMD, for which geometrical data and partitioning curves are available, will be investigated. Thus, the performance of the model can be assessed. Furthermore, in real drums a suspension is used as medium. This enables sedimentation effects, which might influence the separation process.

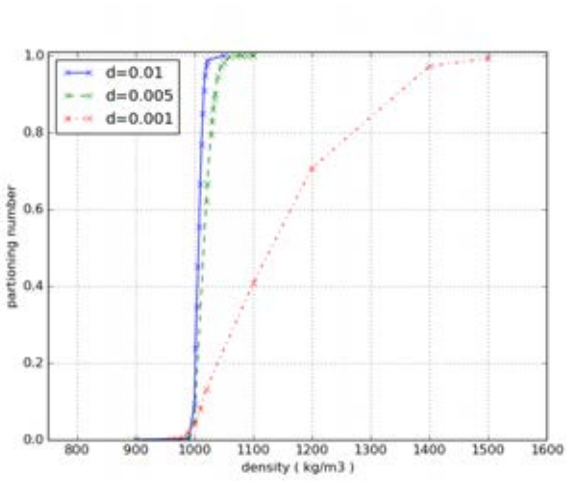

Figure 7: Partitioning curves of the generic DMD for different object diameters.

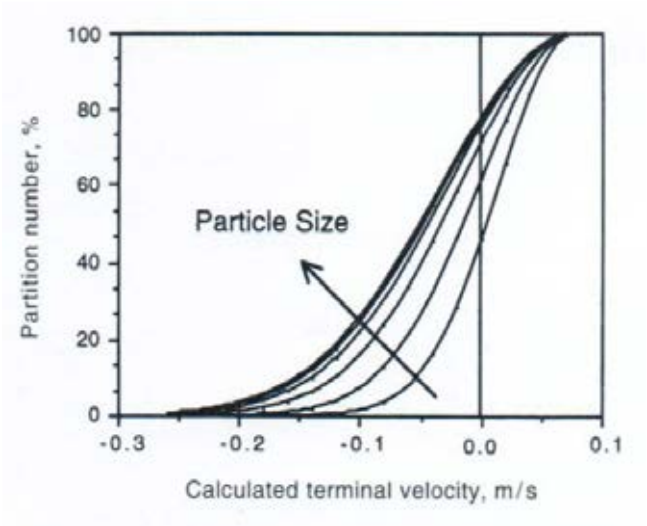

Figure 8: Typical S-shape of a drum separation curve and the influence of different object diameters on it (P.J. Baguley and T.J. Napier-Munn, 1996).

REFERENCES

C. W. Hirt and B.D. Nichols (1981). "Volume of Fluid (VOF) Method for the Dynamics of Free Boundaries". *Journal of Computational Physics*, **39**, 201–225.

DEHBI, A. (2008). "A CFD model for particle dispersion in turbulent boundary layer flows". *Nuclear Engineering and Design*, **238(3)**, 707–715.

DODBIBA, G., HARUKI, N., SHIBAYAMA, A., MIYAZAKI, T. and FUJITA, T. (2002). "Combination of sinkâĂŞfloat separation and flotation technique for purification of shredded PET-bottle from PE or PP flakes". *International Journal of Mineral Processing*, **65(1)**, 11–29.

G. Houzeaux, C. Samaniego, H. Calmet, R. Aubry, M. Vazquez and P. Rem (2010). "Simulation of Magnetic Fluid Applied to Plastic Sorting". *The open Waste Management Journal*, **3**, 127–138.

GOSMAN, A.D. and LOANNIDES, E. (1983). "Aspects of Computer Simulation of Liquid-Fueled Combustors". *Journal of Energy*, **7(6)**, 482–490.

KING, R.P. (1999). "Practical Optimization Strategies for Coal-washing Plants". *Coal Preparation*, **20(1-2)**, 13–34.

KUANG, S., QI, Z., YU, A., VINCE, A., BARNETT, G. and BARNETT, P. (2014). "CFD modeling and analysis of the multiphase flow and performance of dense medium cyclones". *Minerals Engineering*, **62**, 43–54.

MENTER, F.R. (1994). "Two-equation eddy-viscosity turbulence models for engineering applications". *AIAA Journal*, **32(8)**, 1598–1605.

MEYER, E. and CRAIG, I. (2015). "Dynamic model for a dense medium drum separator in coal beneficiation". *Minerals Engineering*, **77**, 78–85.

Napier-Munn (1991). "Modelling and Simulating Dense Medium Seperation Processes - A Progress Report". **4**, 329–346.

Omno Ubbink (1997). *Numerical prediction of two fluid system with sharp interfaces*. Ph.D. thesis, Imperial College of Science, Technology & Science.

P. J. Roache (1994). "Perspective: A Method for Uniform Reporting of Grid Refinement Studies". *Journal of Fluids Engineering*, **116**, 405–413.

P.J. Baguley and T.J. Napier-Munn (1996). "Mathematical model of the dense-medium drum". **105(Jan-April)**, C1–C8.

Stanley Osher and James A. Sethian (1988). "Fronts Propagating with Curvature-Depndent Speed: Algorithms Basd on Hamilton-Jacobi Formulations". *Journal of Computational Physics*, **79**, 12–49.